

Simulation of Aerosol Dynamics: A Comparative Review of Algorithms Used in Air Quality Models

*Yang Zhang**, *Christian Seigneur*, *John H. Seinfeld*,
Mark Z. Jacobson, and *Francis S. Binkowski*

ATMOSPHERIC & ENVIRONMENTAL RESEARCH, INC., 2682 BISHOP DRIVE,
SUITE 120, SAN RAMON, CA 94583 (Y.Z., C.S.),
CALIFORNIA INSTITUTE OF TECHNOLOGY 1200 E. CALIFORNIA BLVD.,
MAIL CODE 104-44, PASADENA, CA 91125 (J.H.S.), STANFORD UNIVERSITY,
DEPARTMENT OF CIVIL AND ENVIRONMENTAL ENGINEERING,
STANFORD, CA 94305 (M.Z.J.), NATIONAL OCEANIC AND
ATMOSPHERIC ADMINISTRATION, ON ASSIGNMENT TO THE U.S.
ENVIRONMENTAL PROTECTION AGENCY, ATMOSPHERIC MODELING DIVISION
(MD-80), NATIONAL EXPOSURE RESEARCH LAB, U.S. EPA,
RESEARCH TRIANGLE PARK, NC 27711 (F.S.B.)

ABSTRACT. A comparative review of algorithms currently used in air quality models to simulate aerosol dynamics is presented. This review addresses coagulation, condensational growth, nucleation, and gas/particle mass transfer. Two major approaches are used in air quality models to represent the particle size distribution: (1) the sectional approach in which the size distribution is discretized into sections and particle properties are assumed to be constant over particle size sections and (2) the modal approach in which the size distribution is approximated by several modes and particle properties are assumed to be uniform in each mode. The sectional approach is accurate for coagulation and can reproduce the major characteristics of the evolution of the particle size distribution for condensational growth with the moving-center and hybrid algorithms. For coagulation and condensational growth, the modal approach provides more accurate results when the standard deviations of the modes are allowed to vary than it does when they are fixed. Predictions of H_2SO_4 nucleation rates are highly sensitive to environmental variables and simulation of relative rates of condensation on existing particles and nucleation is a preferable approach. Explicit treatment of mass transfer is recommended for cases where volatile species undergo different equilibrium reactions in different particle size ranges (e.g., in the presence of coarse salt particles). The results of this study provide useful information for use in selecting algorithms to simulate aerosol dynamics in air quality models and for improving the accuracy of existing algorithms.

*Corresponding author.

INTRODUCTION

Air quality regulations for ambient levels of particulate matter (PM) and regional haze require relating sources of emissions of PM and PM precursors to PM levels and visibility degradation. To that end, three-dimensional (3-D) air quality models of PM have been developed that contain comprehensive treatment of transport processes, gas-phase chemistry, gas/particle partitioning, and aerosol dynamics (Seigneur et al. 1999). These models differ in their treatment of these various atmospheric processes, and it is of interest to assess to what extent differences in model formulations may affect model predictions. We focus here on the algorithms that are used to simulate aerosol dynamics, i.e., those processes that govern the evolution of the particle size distribution. The relevant aerosol dynamic processes include coagulation, condensational growth (or shrinkage due to volatilization), nucleation, and mass transfer from the bulk gas phase to the particle surface. We review the algorithms that are currently used in the following 3-D PM air quality models: CIT (Meng et al. 1998), GATOR (Jacobson 1997a), Models-3/CMAQ (Binkowski and Shankar 1995; Binkowski 1998), SAQM-AERO (Dabdub et al. 1998), UAM-AERO (Lurmann et al. 1997), and UAM-AIM (Sun and Wexler 1998).

First, we present an overview of the 2 major approaches used to represent the particle size distribution in PM air quality models: the sectional approach and the modal approach. Next, we present our comparison of algorithms used to simulate the 4 dynamic processes listed above. Finally, concluding remarks and recommendations for the selection and improvements of aerosol dynamics algorithms are provided.

REPRESENTATION OF THE PARTICLE SIZE DISTRIBUTION

Several approaches can be used to represent the particle size distribution in an at-

mospheric model. The 3 major approaches include continuous representation, sectional representation, and parameterized modal representation. The continuous representation assumes a continuous size spectrum. The aerosol dynamic equations are solved using the finite element methods (e.g., Varoglu and Finn 1980; Tsang and Brock 1986; Tsang and Huang 1990), which provide the most accurate solution. A number of numerical modules based on a continuous representation have been developed to simulate changes in the particle size distribution including COAGUL (Suck and Brock 1979) and CONFEMM (Tsang and Brock 1983). However, the aerosol dynamic modules with a continuous size representation are computationally demanding and are not currently used in 3-D air quality models. Here we will use modules based on this approach (e.g., COAGUL for coagulation and CONFEMM for condensation) as a benchmark to which other approaches are compared.

The sectional representation is used in several air quality models including CIT, GATOR, SAQM-AERO, UAM-AERO, and UAM-AIM. In the sectional approach, the particle size distribution is approximated by a discrete number of size sections (Gelbard and Seinfeld 1980; Gelbard et al. 1980). This discretization can be conducted based on number, surface area, or volume (or mass), depending on the particle characteristics of interest. For example, Wu et al. (1996) showed that the optical characteristics of particles are better approximated if the discretization is conducted according to the particle surface area rather than the particle volume. Because air quality models are generally designed to conserve mass, the sectional representation of the particle size distribution used in PM models is based on the mass distribution of particles. One must note that if mass is transferred between size sections, only 1 characteristic is conserved when all processes (i.e., coagulation and gas-to-particle conversion) are

simulated. For example, if the sectional representation is expressed to conserve mass, then the number distribution will not satisfy the dynamic equation. The mass size distribution is expressed in the sectional representation as follows.

$$Q_l(t) = \int_{x_{l-1}}^{x_l} q(x, t) dx, \quad l = 1, \dots, L, \quad (1)$$

where $q(x, t)$ is the mass size distribution, x is the logarithm of the particle diameter, t is the time, l is the section number, L is the total number of size sections, and Q_l is the particle mass in size section l .

In the parameterized representation, the particle size distribution is approximated by several analytical functions (generally log-normal distributions) that represent the various modes of the particle population. This modal approach is used in Models-3, where the particle size distribution is represented by 3 modes, each mode being approximated by a log-normal distribution. These 3 modes are an Aitken nuclei mode, an accumulation mode, and a coarse mode. The log-normal approximation allows one to simulate the evolution of both the number and volume (or mass) distributions. The number distribution $n(d, t)$ based on particle diameter d is represented as follows:

$$\begin{aligned} n(d, t) = & \frac{N_n(t)}{(2\pi)^{1/2} \log[\sigma_n]} \\ & \times \exp \left[-\frac{1}{2} \left(\frac{\log[d/d_{N_n}(t)]}{\log[\sigma_n]} \right)^2 \right] \\ & + \frac{N_a(t)}{(2\pi)^{1/2} \log[\sigma_a]} \\ & \times \exp \left[-\frac{1}{2} \left(\frac{\log[d/d_{N_a}(t)]}{\log[\sigma_a]} \right)^2 \right] \end{aligned}$$

$$\begin{aligned} & + \frac{N_c(t)}{(2\pi)^{1/2} \log[\sigma_c]} \\ & \times \exp \left[-\frac{1}{2} \left(\frac{\log[d/d_{N_c}(t)]}{\log[\sigma_c]} \right)^2 \right], \end{aligned} \quad (2)$$

where the subscripts $n, a,$ and c refer to the Aitken nuclei, accumulation, and coarse modes, respectively; $N_n, N_a,$ and N_c represent the total aerosol number concentrations in each mode; $d_{N_n}, d_{N_a},$ and d_{N_c} represent the geometric mean particle diameters; and $\sigma_n, \sigma_a,$ and σ_c are the standard deviations of each mode. In the original formulation of the modal representation, both the geometric mean particle diameters and the standard deviations were allowed to vary with time (see Seigneur et al. 1986; Whitby and McMurry 1997). In the original Models-3 formulation, the standard deviations are constant (Binkowski 1998).

Similarly, the volume distribution is represented as follows:

$$\begin{aligned} V(d, t) = & \frac{V_n(t)}{(2\pi)^{1/2} \log[\sigma_n]} \\ & \times \exp \left[-\frac{1}{2} \left(\frac{\log[d/d_{V_n}(t)]}{\log[\sigma_n]} \right)^2 \right] \\ & + \frac{V_a(t)}{(2\pi)^{1/2} \log[\sigma_a]} \\ & \times \exp \left[-\frac{1}{2} \left(\frac{\log[d/d_{V_a}(t)]}{\log[\sigma_a]} \right)^2 \right] \\ & + \frac{V_c(t)}{(2\pi)^{1/2} \log[\sigma_c]} \\ & \times \exp \left[-\frac{1}{2} \left(\frac{\log[d/d_{V_c}(t)]}{\log[\sigma_c]} \right)^2 \right], \end{aligned} \quad (3)$$

where V_n , V_a , and V_c represent the total particle volumes in each mode and d_{V_n} , d_{V_a} , and d_{V_c} represent the geometric mean particle diameters.

SIMULATION OF COAGULATION

Formulation of the Coagulation Algorithms

We compare 2 different approaches that are used in 3-D air quality models to simulate coagulation. The sectional approach is used in several 3-D air quality models for particulate matter; however, only 1 of these models, GATOR, treats coagulation (Seigneur et al. 1998). The modal approach is used in Models-3.

In the sectional approach, the coagulation equation is expressed as follows (Gelbard et al. 1980):

$$\begin{aligned} \frac{dQ_l(t)}{dt} = & \sum_{i=1}^{L-1} \bar{\beta}_{i,l-1} Q_i(t) Q_{l-1}(t) \\ & - \sum_{i=1}^L {}^b \bar{\beta}_{i,l} Q_i(t) Q_l(t), \\ & l = 1, \dots, L. \end{aligned} \quad (4)$$

The first term represents the formation of new particles in section l by coagulation of particles from lower sections, and the second term represents the coagulation of particles from section l with other particles to form particles in higher sections. The sectional coagulation coefficients $\bar{\beta}_{i,l-1}$ and ${}^b \bar{\beta}_{i,l}$ are calculated by integrating the coagulation coefficient $\beta(x_1, x_2)$ over the sections of interest. (See Gelbard et al. (1980) for the derivation of the sectional coagulation coefficients.) The advantage of this sectional method is that for a fixed representation of the aerosol size distribution (i.e., with fixed size sections), the sectional coagulation coefficients are integrated only once and the coagulation equation is then reduced from an integro-differential

equation to a set of ordinary differential equations.

In the modal representation, the coagulation equations consist of a set of 6 ordinary differential equations for the total number and volume concentrations of each mode. The coagulation coefficients used in the Models-3 formulation are described in Appendix A1 of Binkowski and Shankar (1995).

Simulation Results

We evaluate each approach with respect to an accurate numerical solution of the coagulation dynamic equation. This accurate solution was obtained using the model COAGUL (Suck and Brock 1979). Seigneur et al. (1986) evaluated the sectional approach and an earlier version of the modal approach against COAGUL. Since no modifications have been made to the fundamental equations for the sectional approach, we simply summarize the results presented by Seigneur et al. (1986). An evaluation of the revised modal approach (i.e., as used in Models-3) is presented and its performance is compared to those of the sectional approach and an earlier version of the modal approach.

Three scenarios were considered with initial particle size distributions typical of clear, hazy, and polluted urban conditions. The characteristics of these particle size distributions are presented in Table 1. The total PM mass concentrations (assuming a particle density of 1.8 g cm^{-3}) are 11, 57, and $126 \mu\text{g m}^{-3}$ for clear, hazy, and urban conditions, respectively. Simulations were conducted for 12 h for the 3 types of atmospheric conditions.

As shown by Seigneur et al. (1986), little coagulation takes place under clear and hazy conditions. Consequently, we discuss here primarily the results of the simulation of urban conditions, since this simulation

TABLE 1. Initial log-normal size distributions used in the aerosol dynamics model simulations (after Seigneur et al. 1986).

Parameter ^a	Conditions		
	Clear	Hazy	Urban
Mean diameter (μm)			
d_n	0.03	0.044	0.038
d_a	0.2	0.24	0.32
d_c	6.0	6.0	5.7
Standard deviation			
σ_n	1.8	1.2	1.8
σ_a	1.6	1.8	2.16
σ_c	2.2	2.2	2.21
Total volume ($\mu\text{m}^3 \text{cm}^{-3}$)			
V_n	0.03	0.09	0.63
V_a	1.0	5.8	38.4
V_c	5.0	25.9	30.8

^aSubscripts *n*, *a*, and *c* refer to nuclei, accumulation, and coarse modes, respectively.

represents the most stringent test for coagulation algorithms. Figure 1 shows the initial particle size distributions and the particle size distributions simulated after 12 h for urban conditions by COAGUL (i.e., the “exact” solution), the sectional approach using 12 sections between 0.001 and

10 μm , and the modal approach as it is formulated in Models-3.

The sectional approach appears to be fairly accurate. The absolute error averaged over the entire size distribution was at most 3% (Seigneur et al. 1986). The computational burden associated with the sectional simulation of coagulation can be managed effectively by using noniterative numerical techniques (e.g., Jacobson and Turco 1995).

Because the Models-3 formulation assumes fixed standard deviations, the evolution of the particle size distribution is characterized by a shift of the accumulation mode toward larger particle sizes. For example, we see in Figure 1 that the accurate numerical solution of COAGUL does not show any significant shift in the mean particle diameter of the accumulation mode but, rather, shows a decrease in the standard deviation of the accumulation mode. Therefore, the assumption of fixed standard deviations in the Models-3 formulation forces an evolution of the particle size distribution undergoing coagulation that is

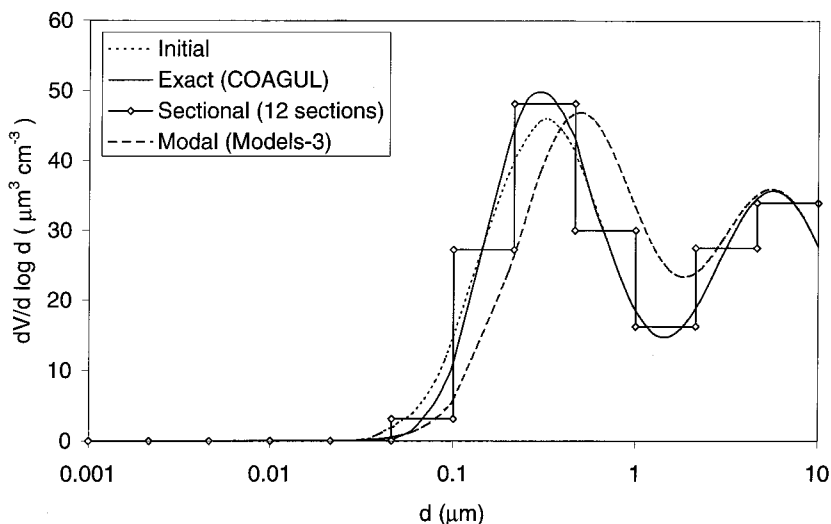


FIGURE 1. Simulation of coagulation for urban conditions, particle volume distributions, initially and after 12 h.

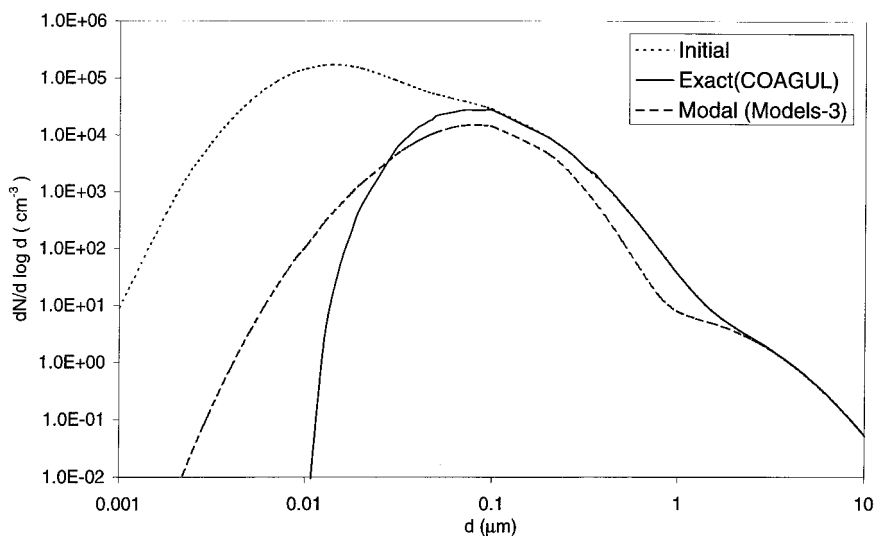


FIGURE 2. Simulation of coagulation for urban conditions, particle number distributions, initially and after 12 h.

not consistent with the evolution calculated with an accurate solution of the coagulation equation.

Figure 2 shows the evolution of the number distribution for the urban simulation. The COAGUL simulation shows a significant depletion of particles below $0.01 \mu\text{m}$, whereas the Models-3 simulation shows a number distribution that is wider with nonnegligible numbers of particles below $0.01 \mu\text{m}$.

We calculated the average absolute error over the diameter range of $0.1\text{--}2.15 \mu\text{m}$ (see Table 2). The errors were 3, 35, and 18% after 12 h of simulation for the sec-

tional formulation, the Models-3 modal formulation, and the original modal formulation of E. Whitby (as described in Seigneur et al. 1986), respectively. The latter modal formulation used a variable standard deviation for all the modes, whereas the Models-3 formulation uses a fixed standard deviation. Therefore, the constraint of using a fixed standard deviation leads to larger error.

The computational time for a 12 h simulation using Models-3 on a Compaq Deskpro 2000 with 64 MB RAM is < 1 CPU s. The sectional and the exact approaches require a significantly longer CPU time, rang-

TABLE 2. Comparison of simulation results for coagulation.^a

Model	Average absolute normalized error (%)		
	Clear	Hazy	Urban
Sectional formulation	1	1	3
Modal formulation of Models-3	2	3	35
Modal formulation of E. Whitby	2	2	18

^a COAGUL was used as the reference (i.e., the "exact" solution). The error was calculated over the diameter range $0.1\text{--}2.15 \mu\text{m}$.

ing from 40–350 CPUs and 100–1000 CPUs, respectively, for various cases.

SIMULATION OF CONDENSATIONAL GROWTH

Formulation of the Condensational Growth Algorithms

We compare 4 different approaches that are used in 3-D air quality models to simulate the growth of particles due to condensation of gas-phase species. These 4 approaches can be grouped into 2 major categories according to their representations of the particle size distribution: sectional or modal. In the original applications of the sectional representation, the condensation equation was expressed as follows (Gelbard and Seinfeld 1980; Seigneur 1982):

$$\frac{dQ_l(t)}{dt} = \bar{\phi}_l Q_l(t) + \bar{\phi}_{l-1} Q_{l-1}(t) - \bar{\phi}_l Q_l(t), \quad l = 1, \dots, L, \quad (5)$$

where the second term is not evaluated for $l = 1$. The first term represents the growth of the aerosol volume in section l due to condensation; the second term represents the growth of the aerosol volume from section $(l - 1)$ into section l ; and the third term represents the growth of the aerosol volume from section l into section $(l + 1)$.

The sectional condensation growth terms are calculated from the growth law and the sectional representation. For example,

$${}^a \bar{\phi}_l = \frac{Q_l}{x_l - x_{l-1}} \int_{x_{l-1}}^{x_l} \frac{\phi}{v} dx, \quad (6)$$

where ϕ is the growth law (i.e., dv/dt) and v is the particle volume. These sectional condensation coefficients are calculated once for a sectional representation that is fixed with respect to particle diameter.

Seigneur et al. (1986) evaluated the sectional approach and concluded that in its

original implementation (Gelbard and Seinfeld 1980; Seigneur 1982), it is subject to significant numerical diffusion. Using 12 size sections in the particle diameter range between 0.001 and 10 μm , the average absolute error for the fine particle size distribution could be as much as 35%. When 3 times as many size sections were used, the error could be reduced to 12%, however, the computational cost increased by a factor of 3. This approach is not currently used in 3-D air quality models, although it is still used in 2-D plume models (Hudischewskyj and Seigneur 1989; Seigneur et al. 1997). Several attempts have been made to minimize numerical diffusion, and the 3 approaches that are currently used in 3-D air quality models can be described as follows.

The exact solution to the condensation equation can be obtained by the method of characteristics. For a sectional representation of the size distribution, it corresponds to allowing the boundaries of the size sections to grow at a rate consistent with the growth law. Thus, the only error in the solution is limited to the error due to the discretization (sectionalization) of the particle size distribution. This approach will be referred to as the full-moving approach, since the entire sectional representation of the particle size distribution moves in the particle diameter space as condensation occurs. However, this approach cannot be used in a 3-D air quality model where it is necessary that the particle size distribution in all grid cells be represented by the same particle size discretization; i.e., the size section boundaries must be fixed.

One approach that has been implemented in some air quality models (e.g., UAM-AERO and SAQM-AERO) takes advantage of the full-moving approach while maintaining the constraint that the particle size sections remain fixed when simulating 3-D processes (Lurmann et al.

1997). For small time steps, the effect of condensation on the particle size distribution is solved using the full-moving approach. Then, at specified larger time steps for which transport processes (advection and diffusion), emissions, and deposition take place, the new particle size distributions are redistributed according to the original particle size representation. The redistribution can be done by assuming that the particle volume distribution is constant within each size section or by fitting the sectional distribution by a continuous distribution prior to its redistribution among the original particle size representation. The latter approach is used in UAM-AERO and SAQM-AERO. Some numerical diffusion takes place at that point. This approach will be referred to as the hybrid approach, since it combines the full-moving approach with the fixed size sectional representation. (It differs, however, from the hybrid method used by Jacobson and Turco [1995].)

Another approach that has been implemented in some air quality models (e.g., CIT and UAM-AIM) consists of using a numerical integration scheme that minimizes numerical diffusion when solving the condensation equation. The condensation equation is a hyperbolic partial differential equation that is mathematically similar to the advection equation. Discretizing the particle size distribution in size sections is equivalent to discretizing a modeling domain with a grid. Therefore, numerical schemes that have been developed to solve the advection equation with minimal numerical diffusion can be used to solve the condensation equation. The numerical scheme developed by Bott (1989) has been considered fairly effective for minimizing numerical diffusion and has been used to solve the condensation equation (Dhanyala and Wexler 1996). We will refer to this

approach as the Bott's approach, based on the numerical scheme being used.

Finally, one approach that has been implemented in GATOR takes advantage of the method of characteristics within the fixed size representation (Jacobson 1997b). In this approach, the mass of each particle size section is assigned to a single particle size. This particle size is then allowed to grow as condensation occurs. When this particle size grows out of the section, all particles of that section are transferred into the next section. A new particle size is calculated for that next section by averaging the particle sizes of the particles previously in the section and of those newly transferred. Thus, numerical diffusion is minimized overall. However, in a 3-D model, several particle size distributions are mixed through transport processes and emissions. In that case, an average diameter must be calculated for the size section. The new diameter is calculated as a volume average of the diameters of the various particle populations (e.g., the initial particle population in the grid cell as modified via aerosol dynamic processes and removal processes, particles advected or dispersed from upwind sources, and new emitted particles). At that point, some error occurs due to the averaging process.

The modal approach is used in Models-3. Three modes are used to represent the particle size distribution, but condensation on the coarse mode is assumed to be negligible. The condensation equations consist of a set of 4 ordinary differential equations for the total number and volume concentrations of the nuclei and accumulation modes. The calculation of the condensational growth coefficients used in the Models-3 formulation is described in Appendix A1 of Binkowski and Shankar (1995).

In the Models-3 formulation, condensation on the nuclei mode is solved together with the nucleation and coagulation terms.

The mathematical formulation is such that if nucleation and coagulation are set to 0, no condensation occurs on the nuclei mode; we refer to this version as Models-3 (EPA1). To circumvent this problem, we used 2 approaches. First, we rewrote the computer code of Models-3 to allow condensation on the nuclei mode using the mathematical formulation of Models-3 for condensational growth; we refer to this version as Models-3 (AER). Second, we conducted the calculations including condensation and coagulation; we refer to this version as Models-3 (EPA2). However, this approach can only be used for cases where coagulation does not significantly affect the particle size distribution. Therefore, the implementation referred to as Models-3 (AER) should be the most representative of the formulation of condensation in Models-3. It will be used here in our comparison of the Models-3 modal algorithm with other condensation algorithms. A brief comparison of the 3 implementations described here (i.e., AER, EPA1, and EPA2) will also be presented.

Simulation Results

We evaluate each algorithm with respect to an accurate numerical solution of the condensational growth equation. This accurate solution was obtained using the full-moving approach with a large number (500) of size sections for the particle diameter range between 0.001–10 μm . Allowing the section boundaries to move eliminates numerical diffusion. This technique cannot be used in a 3-D air quality model as described before. It is, however, appropriate here since we are conducting simulations for a single grid cell. The accuracy of the solution was verified by repeating the simulation with twice as many sections and obtaining the same particle size distribution as with 500 sections after 12 h of simulation.

For consistency among the sectional algorithms, the same growth law was used for all 3 sectional algorithms. It represents the rate of growth of a particle using the formula of Fuchs and Sutugin (1971).

$$\frac{dv}{dt} = \frac{4\pi rD}{1 + \left(\frac{1.333Kn + 0.71}{1 + Kn}\right)Kn} v_m P, \quad (7)$$

where r is the particle radius, D is the diffusion coefficient of the condensing vapor, Kn is the Knudsen number equal to λ/r , λ is the mean free path of the condensing vapor, v_m is the molecular volume of the condensing vapor, and P is the ambient vapor pressure of the condensing vapor. We assume here that the equilibrium vapor pressure of the condensing vapor is 0. In Models-3, the growth law is calculated as the harmonic average of a free-molecular growth law and a near-continuum growth law (Binkowski and Shankar 1995).

We simulated 6 scenarios typical of clear, hazy, and polluted urban conditions as shown in Table 1. Sulfuric acid condensation rates were 0.3 and 0.6, 5.5 and 11, and 4.6 and 9.2 $\mu\text{m}^3 \text{cm}^{-3}$ per 12 h, respectively. Although we focus here on condensational growth, the conclusions that result from this work are also relevant to the evolution of the particle size distribution through volatilization processes.

As shown by Seigneur et al. (1986), the scenario for hazy conditions represents the most stringent test for the simulation of condensational growth. Therefore, we focus our discussion on this case. Figures 3 and 4 present the resultant volume and number size distributions, respectively, for hazy conditions. The simulation of hazy conditions is the most difficult test among those presented here because the high condensation rate and the particle size dependence of the growth law lead to a narrow but significant nuclei mode centered around

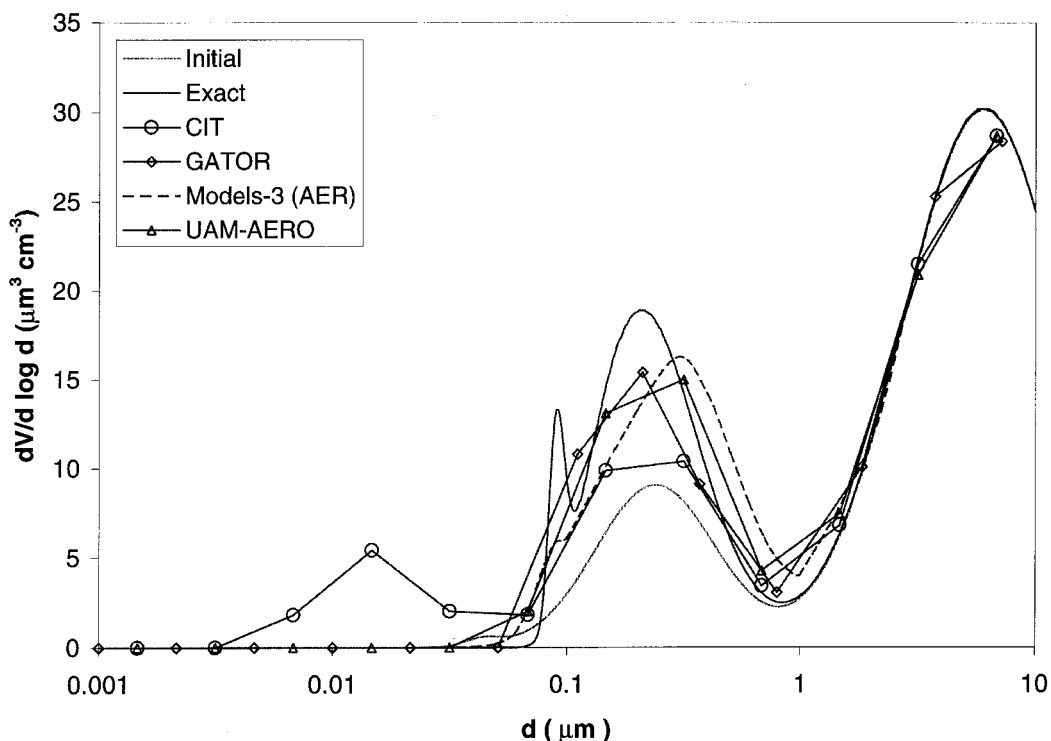


FIGURE 3. Simulations of condensation for hazy conditions with a condensation rate of $5.5 \mu\text{m}^3 \text{cm}^{-3} / 12 \text{ h}$, particle volume distributions, initially and after 12 h.

$0.1 \mu\text{m}$. The “exact” solution obtained with the full-moving algorithm shows a peak of the nuclei mode of about $14 \mu\text{m}^3 \text{cm}^{-3}$; the simulation using the CONFEMM of Tsang and Brock (1983) showed a similar but slightly higher peak of about $17 \mu\text{m}^3 \text{cm}^{-3}$, also centered at $0.1 \mu\text{m}$ (Figure 6; Seigneur et al. 1986). Therefore, the nuclei mode has grown both in volume and in size since the mean diameter changed from $0.044 \mu\text{m}$ (see Table 1) to $0.1 \mu\text{m}$. The accumulation mode increased significantly in volume but its mean diameter decreased from $0.24 \mu\text{m}$ (see Table 1) to about $0.2 \mu\text{m}$. This decrease is due to the fact that the number of particles available for condensation increases steadily as the diameter decreases from $1 \mu\text{m}$ to $0.05 \mu\text{m}$; there-

fore, more condensation occurs on the smaller particle population.

The moving-center algorithm cannot reproduce the narrow nuclei mode centered at $0.1 \mu\text{m}$ because the sectional size resolution is not fine enough. It takes about 100 size sections over the range of 0.001 to $10 \mu\text{m}$ (i.e., a resolution 8 times finer than the one used here) to be able to reproduce this nuclei mode. The moving-center algorithm reproduces the accumulation mode well, although it predicts a mean diameter that is slightly lower than the one predicted by the “exact” solution. The Bott’s algorithm of CIT significantly overpredicts the particle volume below $0.1 \mu\text{m}$. Consequently, mass conservation leads to a significant underprediction of the volume

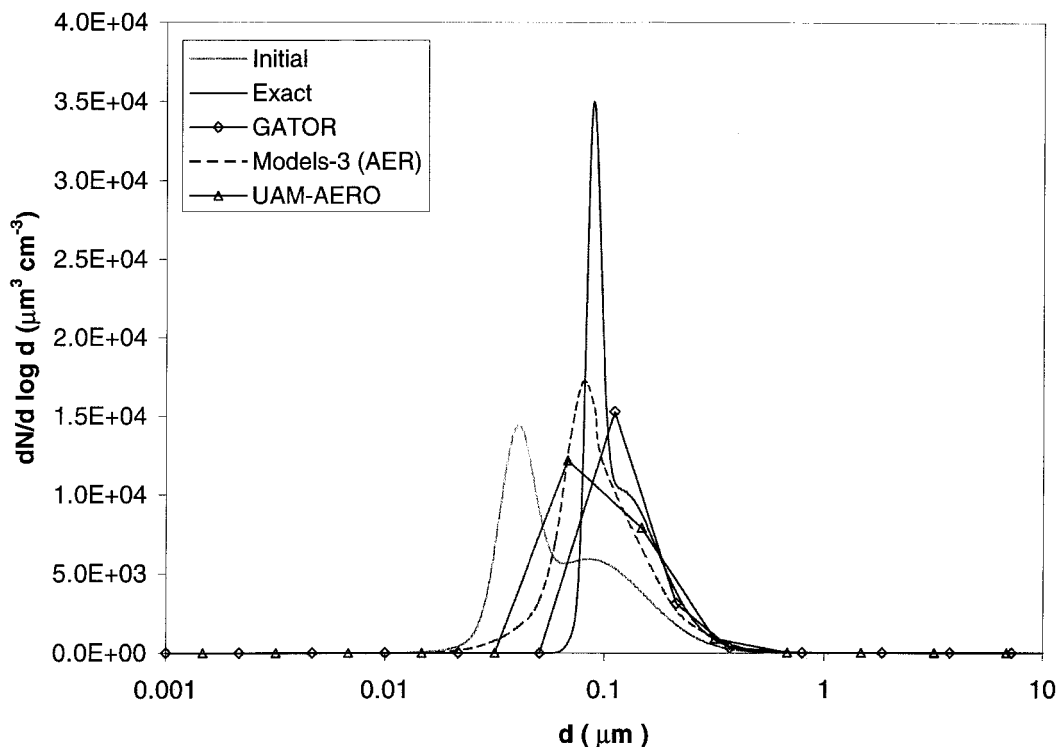


FIGURE 4. Simulations of condensation for hazy conditions with a condensation rate of $5.5 \mu\text{m}^3 \text{cm}^{-3} / 12 \text{ h}$, particle number distributions, initially and after 12 h.

growth in the accumulation mode since most of the condensational growth occurs below $0.1 \mu\text{m}$.

The hybrid algorithm of UAM-AERO reproduces the overall growth of the size distribution well, although it fails to simulate the 2 distinct peaks of the nuclei and accumulation modes that appear in the “exact” solution because of insufficient size resolution in the sectional representation. However, the hybrid algorithm of UAM-AERO may lead to significant numerical diffusion for time steps commensurate with 3-D transport (i.e., less than 1 h).

The Models-3 algorithm does not reproduce the major characteristics of the particle size distribution after 12 h of simulation. The distinct nuclei mode is not

reproduced because the fixed standard deviation assumed in Models-3 does not allow the prediction of such a narrow nuclei mode. The original version of the modal approach of E. Whitby reproduced this narrow nuclei mode very well because it used a variable standard deviation (Seigneur et al. 1986). After 12 h, the accumulation mode shows a mean diameter of about $0.3 \mu\text{m}$. This increase in the mean diameter is due to the fixed standard deviation assumed in the Models-3 formulation. It is not, however, consistent with the results obtained with the full-moving algorithm and CONFEMM, which show a decrease in the mean diameter of the accumulation mode.

The number size distributions show that all algorithms fail to reproduce the sharp

peak that is simulated with the “exact” solution at about $0.1 \mu\text{m}$. This peak value in the number distribution corresponds to the nuclei mode. The sectional algorithms cannot reproduce this peak because the sectional size resolution is too coarse (as mentioned above, it would take a resolution about 8 times finer than the one used here to properly simulate that peak). Among the sectional algorithms, GATOR comes the closest to reproducing that peak. The Models-3 modal algorithm simulates a peak similar to GATOR’s peak in magnitude but at a lower diameter.

As mentioned above, the same condensation growth law of Fuchs and Sutugin (1971) was used for all sectional algorithms. We investigated whether significant differences

would occur in an algorithm’s performance if the original algorithm’s growth law was used. Figure 5 shows the simulation of hazy conditions with the Bott’s algorithm using both the Fuchs–Sutugin growth law and the growth law originally used in CIT (Meng et al. 1998). The performance of the Bott’s algorithm is slightly better when the original CIT growth law is used. However, the discrepancy between the 2 CIT simulations is due primarily to different integration time steps rather than to the mathematical formulation of the growth law. The Fuchs–Sutugin growth law triggers smaller integration time steps compared to the original CIT growth law. Consequently, the numerical errors associated with the Bott’s algorithm accumulate more when using the

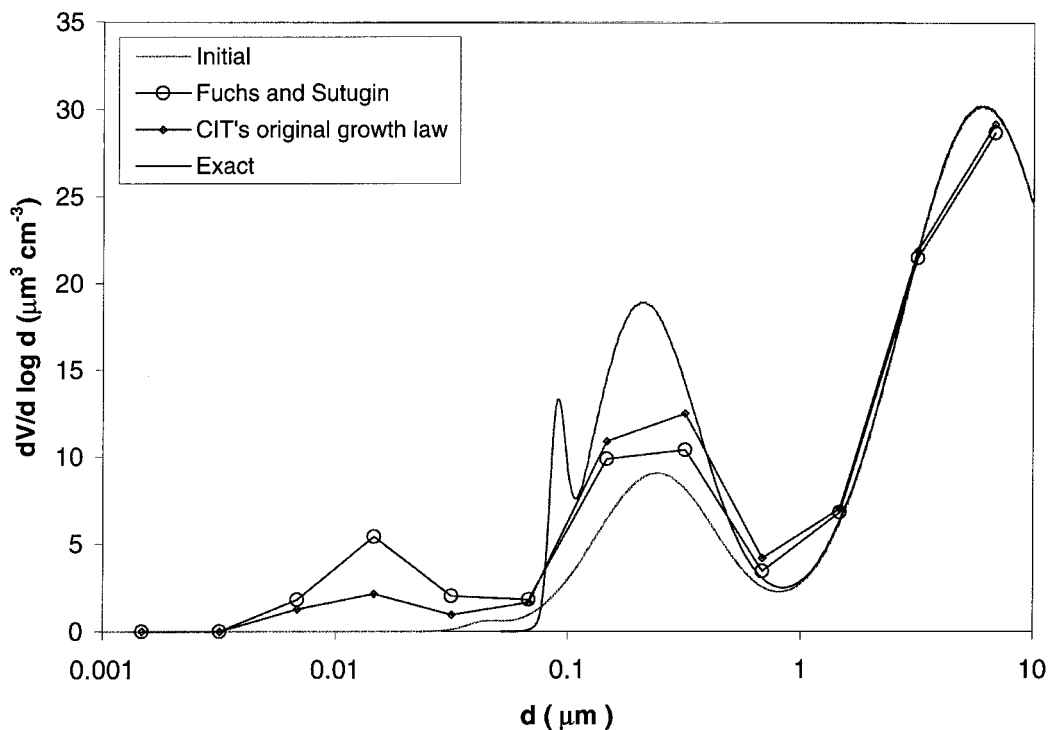


FIGURE 5. Simulations of condensation for hazy conditions using different growth laws with a condensation rate of $5.5 \mu\text{m}^3 \text{cm}^{-3} / 12 \text{ h}$, particle volume distributions, initially and after 12 h.

Fuchs–Sutugin growth law, leading to larger errors in the volume size distribution after 12 h of simulation.

As mentioned above, several implementations of the modal algorithm were considered here under the Models-3 formulation.

- Models-3 (AER): Implementation by AER of changes to the Models-3 mathematical formulation in the Models-3 code (i.e., condensation on the nuclei and accumulation modes).
- Models-3 (EPA1): Application of the Models-3 formulation without nucleation and coagulation (condensation on the accumulation mode only).
- Models-3 (EPA2): Application of the Models-3 formulation without nucleation (condensation on the nuclei and accumulation modes, but with coagulation).

The first algorithm should represent more accurately the formulation of the modal approach in Models-3 and it was used in the simulation results presented in Figures 3 and 4. In Figure 6 we present the volume size distributions simulated with the 3 different implementations of the Models-3 condensation algorithms. As expected, the EPA1 implementation underpredicts particle growth since condensation on the nuclei mode is not simulated; it is, therefore, not a good representation of the actual formulation of Models-3. The AER implementation and the EPA2 implementation give similar results, but the latter implementation leads to slightly higher particle diameter due to coagulation. These results confirm our understanding of the Models-3 formulation and suggest that the AER im-

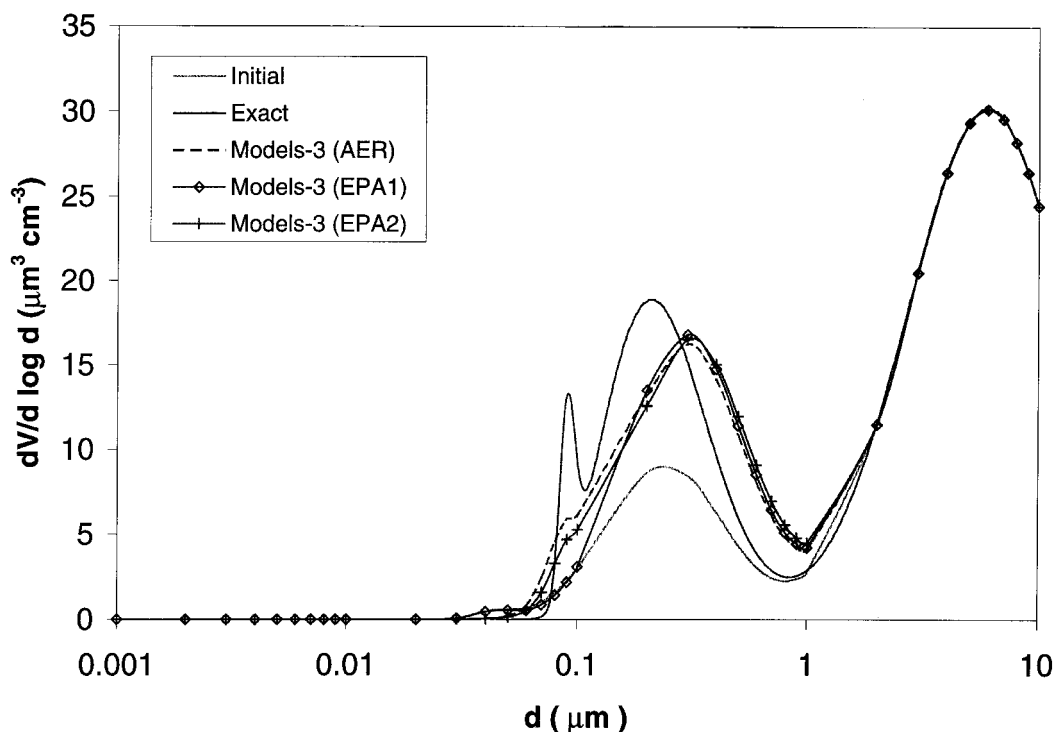


FIGURE 6. Simulations of condensation for hazy conditions using different implementations of the Models-3 algorithm with a condensation rate = $5.5 \mu\text{m}^3 \text{cm}^{-3} / 12 \text{h}$, particle volume distributions, initially and after 12 h.

plementation used above in the algorithm comparison provides a realistic representation of the formulation of condensation in Models-3.

We calculated the average absolute normalized error over the diameter range 0.1–2.15 μm (see Table 3). Over all simulations, the maximum normalized errors were 31, 12, 58, and 21% after 12 h of simulation for CIT (using the Fuchs–Sutugin growth law), GATOR, Models-3 (using the AER implementation), and UAM-AERO, respectively. The original modal formulation of E. Whitby with variable standard deviations (as described in Seigneur et al. (1986)) led to less error (18%) than the current Models-3 modal representation.

The computational time for various condensational growth algorithms varies with the applications studied, the size representations used, and the condensational growth equations used. For a 12-section representation with the Fuchs and Sutugin growth law and a sulfuric acid condensation rate of 11 $\mu\text{m}^3 \text{cm}^{-3}$ per 12 h for hazy conditions, the computational times for the moving-center algorithm, the Bott's algorithm of CIT, and the hybrid algorithm of UAM-AERO are 0.8, 6.2, and 0.1 CPU s, respectively, on a Compaq Deskpro 2000. The computational time for the modal approach of Models-3 is 0.2 CPU s.

SIMULATION OF NUCLEATION

Formulation of Nucleation Algorithms

We compare algorithms used to calculate nucleation of sulfuric acid (H_2SO_4) particles in current 3-D air quality models for particulate matter. Table 4 summarizes the parameterizations used to simulate the rate of nucleation of new particles in air quality models. It is interesting to note that all parameterizations are based on the same set of calculations of nucleation rates performed by Jaeger-Voirol and Mirabel (1989). Therefore, discrepancies in the nucleation rates originate from the algorithms used to parameterize these original calculations. The work of Jaeger-Voirol and Mirabel (1989) is based on heteromolecular homogeneous nucleation theory of H_2SO_4 – H_2O . Jaeger-Voirol and Mirabel present their calculations of nucleation rates as a set of 5 figures that show the nucleation rate as a function of the gas-phase concentration of H_2SO_4 , temperature (223–373 K), and relative humidity (20–100%).

The formulation of H_2SO_4 nucleation rates, as they are currently implemented in 3-D air quality models, can be considered as containing 2 components: (1) The overall formulation that defines whether the nucleation rate is calculated after the condensation rate on existing particles, before the

TABLE 3. Comparison of simulation results for condensation.^a

Initial particle concentration	Average absolute normalized error (%)					
	Clear conditions		Hazy conditions		Urban conditions	
Condensation rate ($\mu\text{m}^3/\text{cm}^3$ per 12 h)	0.3	0.6	5.5	11	4.6	9.2
CIT (the Bott's algorithm)	4	9	17	31	2	4
GATOR (the moving center algorithm)	6	10	12	12	2	3
Models-3 (the modal algorithm, AER version)	6	17	33	58	6	13
UAM-AERO (hybrid algorithm)	9	13	8	21	5	4

^a The average absolute normalized error is calculated with respect to the "exact" solution (full moving algorithm with 500 sections) over the particle diameter range 0.1–2.15 μm .

TABLE 4. Nucleation parameterizations used in 3-D air quality models for particulate matter.

Air quality model	Overall approach	Parameterization for nucleation rate ^a
CIT	Gas-phase H ₂ SO ₄ concentration calculated from SO ₂ oxidation at each time step, nucleation rate calculated before condensation.	Wexler et al. 1994
GATOR	Gas-phase H ₂ SO ₄ concentration calculated from SO ₂ oxidation, nucleation, diffusion-limited condensation simultaneously.	1. Fitzgerald et al. 1998 2. Pandis et al. 1994
Models-3	Gas-phase H ₂ SO ₄ concentration calculated from SO ₂ oxidation and diffusion-limited condensation; nucleation rate calculated next.	1. Harrington and Kreidenweis 1998 2. Kerminen and Wexler 1994
SAQM-AERO	Condensation only	None
UAM-AERO	Condensation only	None
UAM-AIM	Condensation only	None

^a Some models offer alternative parameterizations; the first one listed is the one implemented most recently and is the preferred one.

condensation rate, or together with the condensation rate; and (2) the actual parameterization of the nucleation rate.

In CIT, the nucleation rate is calculated before the condensation rate. After completion of the integration of the gas-phase chemical kinetic equations, the amount of gas-phase H₂SO₄ produced by SO₂ oxidation is updated. This gas-phase H₂SO₄ concentration is then compared to a critical H₂SO₄ concentration to determine what amount (if any) of H₂SO₄ will nucleate. If the gas-phase H₂SO₄ concentration is less than or equal to the critical H₂SO₄ concentration, no nucleation occurs. If the gas-phase H₂SO₄ concentration exceeds the critical H₂SO₄ concentration, the amount of H₂SO₄ in excess of this critical amount nucleates. The amount of H₂SO₄ that does not nucleate condenses on existing particles. Therefore, the amount of H₂SO₄ that nucleates does not depend on the concentrations of existing particles on which condensation may occur. The amount of nucleating H₂SO₄ is placed in the lowest size

section of the particle size distribution (0.039–0.078 μm in the most recent application). The critical concentration of H₂SO₄, [H₂SO₄]_c (μg m⁻³), over which nucleation occurs was developed from the calculations of Jaecker-Voirol and Mirabel (1989) using a nucleation threshold of 1 particle cm⁻³s⁻¹. It is a function of temperature, T (K), and relative humidity, RH (dimensionless fraction), and is expressed as follows (Kerminen and Wexler 1994; Wexler et al. 1994):

$$\begin{aligned}
 [H_2SO_4]_c &= 0.16 \\
 &\times \exp(0.1T - 3.5RH - 27.7).
 \end{aligned}
 \tag{8}$$

In GATOR, the nucleation rate is calculated together with the condensation rate. After solution of the gas-phase chemical kinetic equation over a time integration step, the amount of gas-phase H₂SO₄ produced by SO₂ oxidation is updated. This gas-phase H₂SO₄ concentration is used to estimate a nucleation rate. Then this nucle-

ation rate is converted to a mass transfer rate between the gas and particle phases and is added to the mass transfer rate due to diffusion-limited condensation. Condensation and nucleation are then solved simultaneously (Jacobson 1997b). The number concentration of newly nucleated particles is then extracted from the total particulate mass growth rate and added to the smallest particle size section (0.014–0.024 μm in the most recent application). Since mass-transfer rates due to growth depend on particle number concentration, and condensation is coupled with nucleation, the amount of H_2SO_4 nucleating to form new particles is indirectly affected by the number concentration of existing particles on which condensation occurs.

Two parameterizations of the nucleation rate have been used in GATOR, although homogeneous and heterogeneous classical nucleation rate equations are also present in the model. The original parameterization (hereafter referred to as GATOR1) is based on Pandis et al. (1994) and is for a temperature of 298 K.

$$\log J = 7 + [(-64.24 + 4.7RH) + (6.13 + 1.95RH) \log [\text{H}_2\text{SO}_4]], \quad (9)$$

where J is the nucleation rate in particles $\text{cm}^{-3} \text{s}^{-1}$, RH is in dimensionless fraction, and $[\text{H}_2\text{SO}_4]$ is the gas-phase sulfuric acid concentration. This parameterization is based on the calculated nucleation rates of Jaeger-Voirol and Mirabel (1989) and the use of an experimental nucleation factor proposed by Raes et al. (1992). This parameterization does not provide any temperature dependence.

The new parameterization (hereafter referred to as GATOR2) is based on the work of Fitzgerald et al. (1998) and includes temperature dependence. They developed their parameterization of the

H_2SO_4 nucleation rates based on the calculations of Jaeger-Voirol and Mirabel (1989). Their parameterization depends on the gas-phase H_2SO_4 concentration, RH , and T ; it is intended primarily for $RH > 60\%$.

$$\log J = -2 + \frac{3E}{C} \quad \text{for } E \leq 0, \quad (10)$$

$$\log J = 1 + \frac{3D}{C} \quad \text{for } E > 0, \quad (11)$$

where J is the nucleation rate in particles $\text{cm}^{-3} \text{s}^{-1}$; E and D are functions of the H_2SO_4 gas-phase concentration, RH , and T ; and C is a function of RH and T (C has different formulations depending on the signs of E and D).

In Models-3, the nucleation rate is calculated after the condensation rate. A gas-phase H_2SO_4 concentration is calculated from a steady-state assumption based on gas-phase oxidation of SO_2 to H_2SO_4 and H_2SO_4 condensation or existing particles. This gas-phase H_2SO_4 concentration is then used to calculate the H_2SO_4 nucleation rate.

Two parameterizations of the nucleation rate are available in Models-3. The original parameterization is based on the work of Kerminen and Wexler (1994) and is therefore similar to the parameterization used in CIT. (Note, however, that in CIT the nucleation rate is calculated before the condensation rate.)

The most recent parameterization is based on the work of Harrington and Kreidenweis (1998). This parameterization is also based on the calculations of Jaeger-Voirol and Mirabel (1989). The major difference with the parameterization of Kerminen and Wexler (1994) is that Harrington and Kreidenweis do not make any assumption of a threshold nucleation rate. The parameterization of Harrington and Kreidenweis assumes that the nucleation rate is constant over a time period, and it is

calculated by integrating the time-dependent nucleation rate over that time period. Another difference between the 2 parameterizations is that the parameterization of Harrington and Kreidenweis estimates the nucleation rate for both number and mass, whereas the parameterization of Kerminen and Wexler estimates only the nucleation rate for mass. The parameterization of Harrington and Kreidenweis was used for our comparative evaluation.

Simulation Results

Our comparative evaluation focuses on the nucleation parameterizations. The competition between nucleation of new particles and condensation on existing particles for gas-to-particle conversion is not considered here. Our simulations are therefore representative of an ultraclean atmosphere, and nucleation rates in a typical clear, hazy, or polluted urban atmosphere would be lower due to removal of H_2SO_4 gas molecules via condensation on existing particles. Because some nucleation parameterizations (i.e., CIT and GATOR) require the H_2SO_4 gas-phase concentration, it is necessary to calculate the H_2SO_4 gas-phase concentrations from the H_2SO_4 production rate. To that end, we need to specify an integration time step. Two time steps were used (5 and 15 min) to test the sensitivity of the nucleation rate to the time step specification. Note that in the air quality model implementation, only the CIT nucleation formulation is sensitive to the value of the time step because, in GATOR, the H_2SO_4 gas-phase concentration is calculated from the production and gas-to-particle conversion (i.e., nucleation and condensation) rates.

We compared the nucleation algorithms for a variety of conditions covering H_2SO_4 production rates ranging from $0.045 \mu\text{g m}^{-3} \text{h}^{-1}$ to $1.65 \mu\text{g m}^{-3} \text{h}^{-1}$, relative humidities ranging from 10 to 95%, and ambient

temperatures ranging from 273 to 303 K. No significant nucleation occurred for the low H_2SO_4 production rate. Therefore we focus our discussion on the simulation of the high H_2SO_4 production rate. Results are presented for the smaller time step, i.e., 5 min. Higher nucleation rates were obtained in our simulations for the CIT and GATOR algorithms when using a time step of 15 min (the results of the Models-3 algorithm do not depend on the time step used), but the conclusions were qualitatively similar.

Figure 7 shows the nucleation rates predicted by 4 algorithms as a function of RH for the H_2SO_4 production rate of $1.65 \mu\text{g m}^{-3} \text{h}^{-1}$ and a temperature of 298 K. Also shown on the figure are the maximum H_2SO_4 nucleation rate (labeled $[\text{H}_2\text{SO}_4]$) allowed from the H_2SO_4 production rate. Therefore, in an air quality model simulation, nucleation rates will necessarily be capped at that maximum H_2SO_4 nucleation rate due to mass conservation constraints. The nucleation rate that corresponds to 1% of the maximum nucleation rate is also shown (labeled 1% $[\text{H}_2\text{SO}_4]$); if the calculated nucleation rate is $< 1\%$ of that value, then nucleation is a negligible pathway for H_2SO_4 gas-to-particle conversion because condensation on existing particles would dominate in a pristine environment. Therefore the range between these 2 lines, (H_2SO_4) and 1% $[\text{H}_2\text{SO}_4]$, represents the range of relevant nucleation rates.

All algorithms, except GATOR2 and Models-3, predict nucleation rates that exceed the 1% maximum rate level for some RH values; however, they differ significantly for the range of RH over which nucleation rates are nonnegligible. Both CIT and Models-3 algorithms show little dependence on RH for high RH values. Models-3 predicts a negligible nucleation rate with a sharp decrease in the nucleation rate for $RH < 30\%$. CIT predicts no nucle-

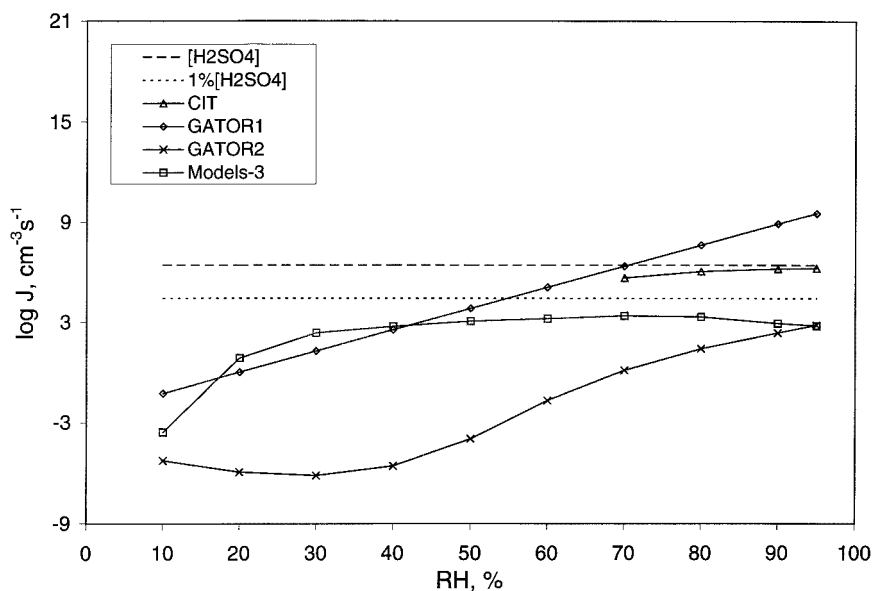


FIGURE 7. Nucleation rate as a function of $RH([H_2SO_4] = 1.65 \mu g m^{-3} h^{-1}, T = 298 K, \text{ and } dt = 5 \text{ min})$.

ation below $RH = 70\%$. For cases where the CIT algorithm predicts that nucleation occurs, it calculates a nucleation rate that is 2–3.5 orders of magnitude greater than the nucleation rate predicted by the Models-3 algorithm. Both GATOR1 and GATOR2 algorithms predict an increase in the nucleation rate with RH , except as RH increases from 10 to 30%, where GATOR2 predicts a slight decrease of the nucleation rate. However, the GATOR1 algorithm predicts a nucleation rate that is up to 8 orders of magnitude greater than the nucleation rate predicted by the GATOR2 algorithm. The GATOR2 algorithm predicts a negligible nucleation rate. At high RH , the highest nucleation rates are predicted by the GATOR1 and CIT algorithms. At low RH , GATOR1 predicts the highest (although negligible) nucleation rate.

Figure 8 shows the predicted nucleation rates for the H_2SO_4 production rate of $1.65 \mu g m^{-3} h^{-1}$ and a RH of 80%, as a

function of temperature (T). Several algorithms show maximum nucleation rates over some temperature range (nucleation rates that are predicted here to exceed the maximum nucleation rate will be capped at that maximum value in an air quality model to maintain mass conservation). Because the GATOR1 algorithm does not include temperature dependence, it predicts a maximum nucleation rate for the whole temperature range. The GATOR2 algorithm predicts a maximum nucleation rate for temperatures $< 280 K$. The CIT algorithm predicts a maximum nucleation rate for most cases, except for $T > 290 K$. The Models-3 algorithm predicts a nucleation rate that is negligible at all temperatures. Discrepancies between the predicted nucleation rates range from 4 orders of magnitude at 273 K to 8 orders of magnitude at 303 K.

Calculations of absolute values of nucleation rates are obviously quite uncertain in light of the results presented here. In a

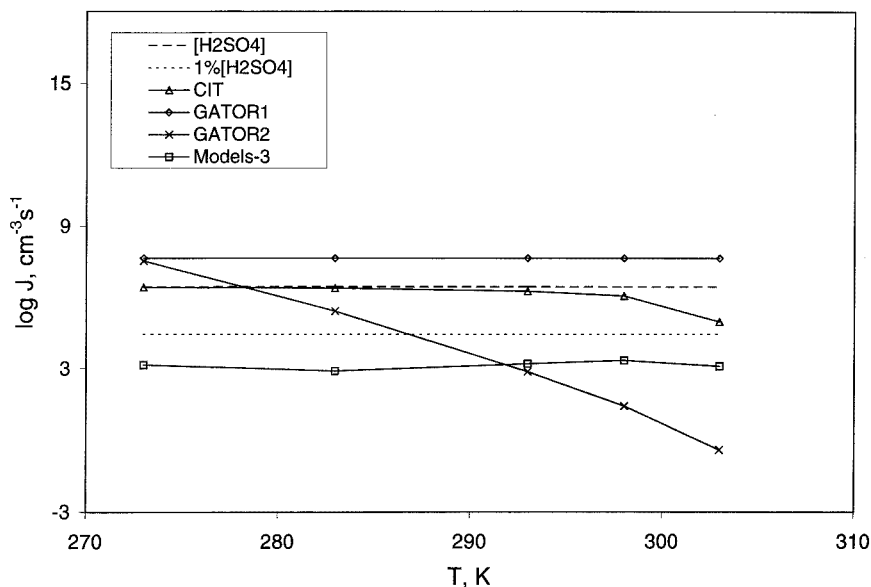


FIGURE 8. Nucleation rate as a function of temperature ($[H_2SO_4] = 1.65 \mu g m^{-3} h^{-1}$, $RH = 80\%$, and $dt = 5$ min).

polluted urban environment, where 3-D air quality models will be applied to address PM-2.5 standard issues, it is appropriate in most cases to assume that nucleation is negligible compared to condensation and can therefore be ignored. An exception may be near strong pollution sources where nucleation rates could be very high (e.g., emission of SO_3 that rapidly hydrolyzes to H_2SO_4). In a nearly pristine environment, where proposed regional haze regulations will apply, it may be appropriate to simulate nucleation. In that case, an approach that partitions gas-to-particle conversion between nucleation of new particles and condensation on existing particles is a better approach than one based on the absolute prediction of a nucleation rate. For example, the work of McMurry and Friedlander (1979) provides some basis for developing such formulations.

Simulation of nucleation using the aforementioned algorithms requires minimal computational time (< 0.1 CPU s on a

Compaq Deskpro 2000) because all these formulations are analytical functions of the H_2SO_4 gas-phase concentration, RH , and/or T .

SIMULATION OF GAS / PARTICLE MASS TRANSFER

Formulation of Gas / Particle Mass Transfer

We compare 3 different approaches to the treatment of mass transfer between the bulk gas phase and the surface of atmospheric particles. These approaches can be summarized as follows:

- Kinetic approach, where mass transfer is simulated explicitly; chemical concentrations in the bulk gas phase and in the particles may or may not be in equilibrium.
- Equilibrium approach, where the bulk gas phase is assumed to be in chemical equilibrium with the particles. All particles

must therefore have the same chemical composition for species involved in gas/particle equilibrium.

- Hybrid approach, where the bulk gas phase is assumed to be in chemical equilibrium with the whole particulate phase, but where the distribution of condensable/volatile species among particles of different sizes is calculated using diffusion-limited assumptions. Although the whole particulate phase is in equilibrium with the gas phase, individual particles (or particles in a given size range) may not be in equilibrium with the gas phase.

The kinetic approach is based on solving the equation for mass transfer between the bulk gas-phase and individual particles (or particle populations). In current 3-D air quality models such as CIT, GATOR, and UAM-AIM, particles are assumed to be internally mixed (i.e., all particles of the same size have the same chemical composition) and are distributed according to size sections (i.e., all particles within a given size range have the same chemical composition). Therefore the mass transfer equation is solved between the bulk gas phase and the surface of the particles. The mass flux J_l of the condensing vapor to the surface of a single particle in size section l can be expressed as follows.

$$J_l = \frac{4\pi rD}{1+F} (C_g - C_{sl}), \quad (12)$$

where r is the particle radius, D is the diffusion coefficient of the condensing vapor in the air, F is a correction factor that accounts for the effect of particle size on condensation rate, C_g is the chemical species concentration in the bulk gas phase, and C_{sl} is the chemical species concentration at the surface of the particles in section l . For large values of r , F tends toward 0 and the flux is proportional to r (continuum regime). For small values of r , F is

proportional to λ/r , where λ is the mean free path of the air and the flux is proportional to r^2 (free-molecule regime). There are various formulations of the function F for the representation of the transition regime between the free-molecule regime (where J is proportional to r^2) and the continuum regime (where J is proportional to r). For example, in the Fuchs–Sutugin (1971) formulation

$$F = \left(\frac{1.333\lambda/r + 0.71}{1 + \lambda/r} \right) \frac{\lambda}{r}; \quad (13)$$

then F tends toward $1.333 \lambda/r$ as r decreases. In CIT, the following formulation is used (Wexler and Seinfeld 1990).

$$F = \frac{\lambda}{\alpha r}, \quad (14)$$

where α is the accommodation coefficient of the chemical species on the particle (i.e., probability that the chemical species will remain on the particle). The CIT factor was used in our simulations.

At the particle surface, the gas-phase concentration is in equilibrium with the particle-phase concentration.

$$K = \frac{C_{pl}}{C_{sl}}, \quad (15)$$

where K is the thermodynamic equilibrium constant (e.g., Henry's law constant for gas/liquid equilibrium) and C_{pl} is the chemical species concentration in the particle. For a multicomponent mixture, concentrations in the liquid particulate phase are corrected for nonideality of the solution using activity coefficients. In CIT, chemical equilibrium between the particles and the gas phase is calculated using the SCAPE2 module (Meng et al. 1998).

Next, it is necessary to calculate the growth of particles from section $(l-1)$ to section l , and from section l to section

($l + 1$), due to the condensational growth of particles. Several numerical algorithms are available to calculate the mass flux from one size section to the next. Bott's scheme is used to solve the condensational growth equation in CIT (Bott 1989; Dhaniyala and Wexler 1996).

If volatilization occurs instead of condensation, the above processes are simulated in reverse with a mass flux from the particle surface toward the bulk gas phase and shrinkage of the particle as chemical mass is transferred from the particle phase to the gas phase.

The equilibrium approach is used in Models-3 (Binkowski and Shankar 1995; Binkowski 1998) and in models that do not provide a resolution of particle chemical composition as a function of particle size. For example, model simulations where only one section is used to represent the particle population, such as the applications of SAQM-AERO to the California San Joaquin Valley (Dabdub et al. 1998) or the Los Angeles Basin, CA (Pai et al. 1998), involve an equilibrium approach. The equilibrium approach is also used with a sectional size distribution in plume models (Hudischewskyj and Seigneur 1989; Seigneur et al. 1997).

In the equilibrium approach, the mass transfer between the bulk gas phase and the particle surface is assumed to be instantaneous so that there is no concentration gradient between the bulk gas phase and the particle surface.

$$C_{sl} = C_g, \quad l = 1, \dots, L. \quad (16)$$

Then all particles are in equilibrium with the same gas-phase chemical concentration.

$$K = \frac{C_{pl}}{C_g}. \quad (17)$$

Consequently, all particles have the same chemical composition.

$$C_{pl} = C_p, \quad l = 1, \dots, L. \quad (18)$$

The hybrid approach was originally introduced by Pandis et al. (1994) and later implemented by Lurmann et al. (1997) in UAM-AERO and SAQM-AERO. A hybrid approach has also been implemented as an option in CIT (Meng et al. 1998). In the hybrid approach, equilibrium is assumed between the bulk gas phase (C_g) and the whole particulate phase. Let Q_l be the mass of particles in section l , and let C_{pl} be the concentration (per unit mass of particle) of the chemical species of interest in particles in size section l . Then the following equilibrium relationship is assumed:

$$K = \frac{\sum Q_l C_{pl}}{\sum Q_l} \frac{1}{C_g}. \quad (19)$$

However, each size section is not required to be in individual equilibrium with the bulk gas phase. Instead, the condensing chemical species is distributed among the size sections according to the flux relationship defined in Equation (12).

The hybrid approach used in UAM-AERO differs slightly from the option available in CIT. In UAM-AERO, the amount of water present in the particles is calculated through an equilibrium relationship that is specific to each particle size section. The simulation results presented here focus on the size distribution of sulfate, nitrate, ammonium, sodium, and chloride species, and we use the hybrid approach available in CIT.

Simulation Results

The kinetic approach provides the most comprehensive solution to the gas/particle conversion process. To ensure that differences in the results are due only to the

treatment of mass transfer, simulations were conducted with the same aerosol module for thermodynamic equilibrium (SCAPE2) and condensational growth (CIT algorithm).

The CIT mass transfer module was used to represent the kinetic approach. The hybrid approach was simulated within CIT by using the same conceptual approach as used in the UAM-AERO mass transfer module. The equilibrium approach was simulated by assuming gas/particle equilibrium and the same particulate chemical composition of volatile compounds for all particle sizes.

Simulations were conducted for 4 different sets of atmospheric conditions. The emphasis was placed on addressing different conditions that affect mass transfer, i.e., various aerosol size distributions and size-resolved chemical compositions. The list of these conditions is presented in Table 5. The PM size-resolved chemical composition affects the local thermodynamic equilibrium of each particle (or, in our case, particle size section). The particle size distribution affects the distribution of condensable species to various particle sizes (or, alternatively, the volatilization of chemical species from the various particle sizes). The concentrations of condensable species will affect the importance of the kinetics of the mass transfer process. Simulations were conducted for 15 h to provide enough time for the mass transfer to take place.

The first 2 cases are intended to represent conditions typical of the Los Angeles Basin, where it has been demonstrated that neglecting the mass transfer kinetics makes a difference on the particulate concentrations. A major question is whether it will make a difference in other areas of the country and, if it does, what the uncertainty associated with neglecting the mass transfer kinetics is. Therefore, the next 2 cases are representative of conditions in the cen-

tral U.S., where there is no significant amount of sodium chloride in the particulate phase and the nitrate concentrations are lower.

The results are shown in Figures 9 and 10 for the 2 cases listed in Table 5 that have high ammonia concentrations (i.e., more ammonium nitrate condensation). In each figure, the results are presented for the size-distributed chemical composition for the kinetic approach after equilibrium has been reached (i.e., particulate nitrate concentration within 1% of equilibrium value), the hybrid approach, and the equilibrium approach. The time needed to reach equilibrium with the kinetic approach is also indicated.

More time is needed to reach equilibrium when HNO_3 reacts with NaCl to form particulate nitrate in coarse particles because it takes large particles longer than small particles to reach equilibrium with the bulk gas phase (Wexler and Seinfeld 1990; Meng and Seinfeld 1996). Also, the kinetic approach leads to more nitrate present in coarse particles than in the equilibrium and hybrid approaches, and the peak of the particle size distribution differs among the 3 approaches.

When no NaCl is present, ammonium nitrate condenses on fine particles and equilibrium is reached fairly rapidly. After 1 h, the kinetic approach predicts that at least 74% of ammonium nitrate has already condensed. The hybrid approach gives a size distribution similar to the one predicted by the kinetic approach. The equilibrium approach, however, predicts a slightly different size distribution.

Carbonate salts will have a similar effect to chloride salts, as carbonate reacts with acid species such as HNO_3 and H_2SO_4 , leading to the release of CO_2 and the formation of particulate nitrate and sulfate, respectively.

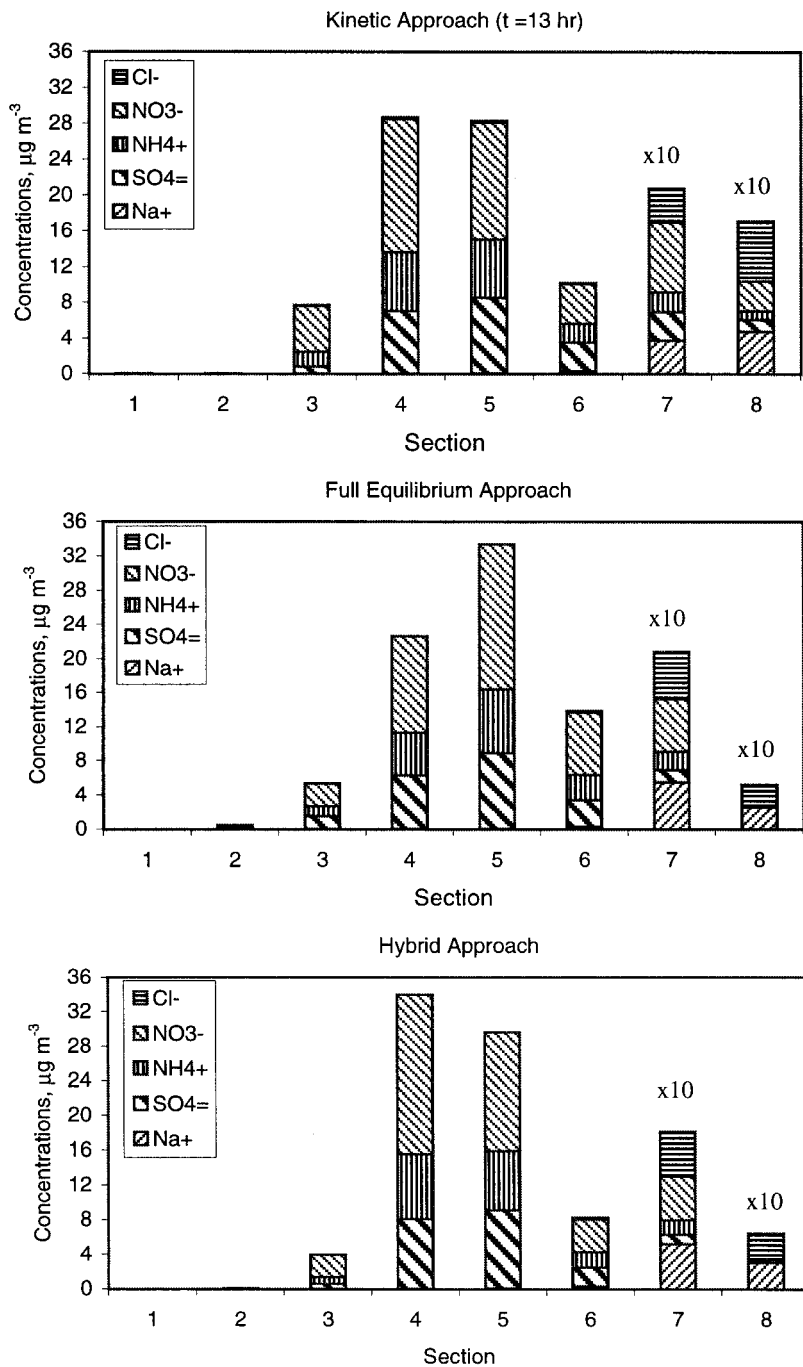


FIGURE 9. Size-resolved equilibrium chemical composition of particles calculated for case 2 at equilibrium with the kinetic, full equilibrium, and hybrid approaches.

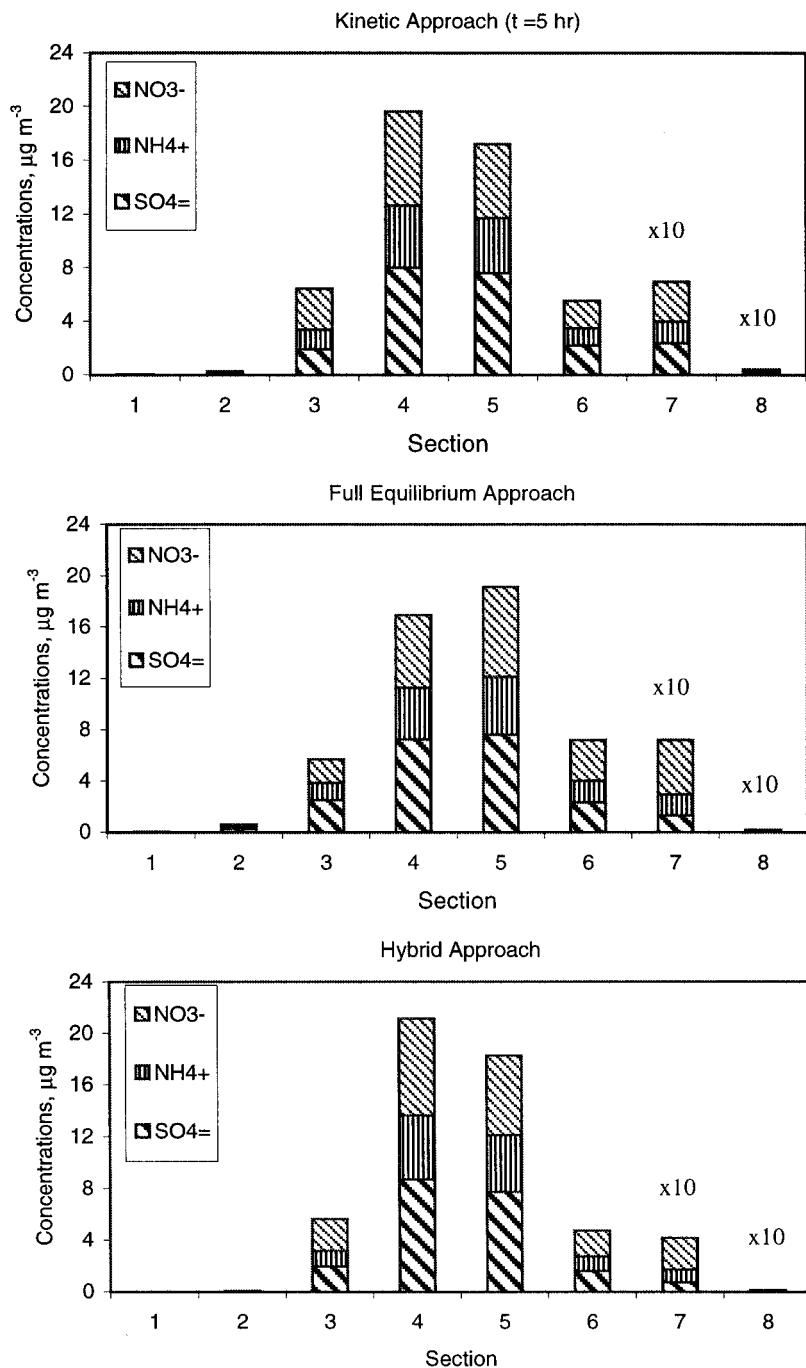


FIGURE 10. Size-resolved equilibrium chemical composition of particles calculated for case 4 at equilibrium with the kinetic, full equilibrium, and hybrid approaches.

TABLE 5. Conditions used for the comparison of kinetic, hybrid, and equilibrium mass transfer approaches (particulate sulfate concentration¹ = 20 $\mu\text{g m}^{-3}$ in all simulations, initial particulate ammonium concentration¹ = 9.7 $\mu\text{g m}^{-3}$, initial particulate nitrate concentration¹ = 7.6 $\mu\text{g m}^{-3}$).

Simulation	HNO ₃ (ppb)	NH ₃ (ppb)	NaCl ($\mu\text{g m}^{-3}$) ²
1	15	5	3
2	15	15	3
3	5	5	0
4	5	15	0

¹ Size distribution is assumed to be log-normal with a mass median diameter of 0.3 μm and a standard deviation of 1.8.

² Size distribution is assumed to be log-normal with a mass median diameter of 3 μm and a standard deviation of 2.2.

The computational time varies with the applications studied, the size representations used, and the mass transfer approaches used. For example, for case 4 with an 8-section representation, the equilibrium and the hybrid approaches used < 0.5 CPU s on a Compaq Deskpro 2000 with 64 MB RAM. The kinetic approach used 27 CPU s, a factor about 50 times longer than those of the equilibrium and the hybrid approaches. For cases with chloride and/or carbonate concentrations in coarse particles, the CPU time for the equilibrium and the hybrid approaches is similar to that of cases without chloride and carbonate salts, whereas the CPU time for the kinetic approach increases significantly (by a factor of 5–100 depending on the specific cases) because it takes longer for large particles to reach gas/particle equilibrium.

CONCLUSIONS

We have compared algorithms that are currently used in 3-D air quality models to simulate aerosol dynamics, including coagulation, condensational growth, nucleation,

and gas/particle mass transfer. Our review included aerosol modules used in CIT, GATOR, Models-3, SAQM-AERO, UAM-AERO, and UAM-AIM.

Algorithms available to simulate coagulation and condensational growth can be grouped into 2 major categories according to the representation of the particle size distribution, i.e., sectional or modal. Models-3 uses a modal approach using 3 log-normal distributions with constant standard deviations to represent the Aitken nuclei, accumulation, and coarse modes. Models-3 will be updated to include a modal approach that uses variable standard deviations (Binkowski 1999). The other models use a sectional representation, although they differ in their treatment of the numerical solution to the condensational growth equation and only 1 model (GATOR) simulates coagulation.

Simulation of coagulation with a sectional approach is numerically accurate. The modal approach is not accurate if fixed standard deviations are used; better accuracy is obtained if variable standard deviations are used.

The most accurate solution of the condensational growth equation was obtained with the moving-center algorithm of GATOR. The hybrid algorithm of UAM-AERO shows some numerical diffusion but was able to reproduce the major features of the evolution of the particle size distribution. However, performance of both the moving-center and the hybrid algorithms needs to be evaluated for 3-D model simulations because numerical diffusion may then increase. The Bott's numerical scheme appears to generate unrealistic results for the very small particle size range (i.e., below 0.01 μm). The modal approach can be fairly accurate if the standard deviations of the distributions are allowed to vary but is inaccurate if fixed standard deviations are used.

Very large differences were found among the 4 parameterizations of H_2SO_4 nucleation rates used in CIT, GATOR (2 parameterizations), and Models-3. Absolute values of nucleation rates vary by many orders of magnitude among the 4 algorithms considered here. Moreover, the dependence of these algorithms on RH and temperature varies widely from one algorithm to another. Considering the fact that all 4 algorithms were derived from the same data set of calculations of heteromolecular homogeneous nucleation of $\text{H}_2\text{SO}_4 \cdot n \text{H}_2\text{O}$ (Jaeger-Voirol and Mirabel 1989), these results reflect the extreme sensitivity of nucleation rates to environmental parameters. Therefore, an approach based on the relative rates of nucleation and condensation seems preferable to one that is based on absolute nucleation rates.

Simulation of gas/particle mass transfer for volatile species was performed using an explicit kinetic treatment of mass transfer between the bulk gas phase and the particle surface, an equilibrium between the bulk gas phase and the particles (i.e., instantaneous mass transfer), or a hybrid approach that assumes equilibrium for the whole particulate matter but distributes mass over the particles according to a diffusion-limited condensation algorithm. For areas where compounds containing chloride or carbonate are a significant component of PM, the kinetic approach is recommended because mass transfer from the gas phase to coarse particles is the rate limiting process (e.g., coastal areas for chloride and arid areas for carbonate). For cases where chloride and carbonate compounds are not important, it is appropriate to use the hybrid approach, since it gives results similar to those obtained with the kinetic approach and equilibrium is reached within about an hour.

The selection of size representations and algorithms to simulate various aerosol dynamic processes including coagulation, con-

densation/evaporation, nucleation, and gas/particle mass transfer may depend on the specific objectives of the study. With appropriate numerical algorithms and size resolution, a sectional representation can predict more accurate chemical composition and size distribution than a modal representation; however, it requires more computational time than the modal approach. Therefore, the algorithms based on a detailed sectional representation may be more appropriate for detailed simulations of aerosol dynamics and thermodynamics, whereas a modal approach or a 2-section (fine and coarse) representation may be suitable for large-scale applications where computational efficiency is required. The accuracy of the sectional representation strongly depends on the size resolution, which can be determined based on the specific applications. For example, a sectional representation of 8 size sections over the 0.02–10 μm particle diameter range is generally sufficient to simulate detailed aerosol dynamics and thermodynamics and is thus commonly used in current 3-D air quality models. For visibility studies, such a resolution has been shown to be sufficient to calculate the particle extinction coefficients as long as the proper approach is used to calculate the sectional extinction coefficients (Wu et al. 1996). For regulatory applications pertaining to PM ambient concentrations, a sectional representation with 2 sections (i.e., the fine $\text{PM}_{2.5}$ and the coarse PM_{10} sections) may be sufficient in cases where there is little interaction between the fine and coarse modes (i.e., in the absence of chloride and carbonate).

Further work should address the simulation of these various processes together, for a range of typical atmospheric conditions. One would expect that the overall error will be governed by the coagulation algorithm when gas/particle conversion processes are negligible and by gas/particle conversion

algorithms (growth, shrinkage, and mass transfer) when secondary aerosol formation is significant. Assessing the overall error associated with aerosol dynamic processes will allow us to place uncertainty bounds on air quality model predictions of PM concentrations. All the simulations presented in this work were conducted in a stand-alone mode (i.e., outside of their 3-D host air quality models); further evaluation of the most promising algorithms for aerosol dynamics and thermodynamics is needed in a 3-D gridded setting where emissions, transport, dispersion, and deposition also take place.

This work was supported by the Coordinating Research Council (CRC) under Contract A-21-2. Thanks are due to CRC for constructive comments.

References

- Binkowski, F. S. (1998). EPA Office of Research & Development, Research Triangle Park, NC, private communication.
- Binkowski, F. S. (1999). Aerosols in Models-3 CMAQ. In *Science Algorithms of the EPA Models-3 Community Multiscale Air Quality (CMAQ) Modeling System*, Chapter 10, edited by D. W. Byun and J. K. S. Ching. Office of Research And Development, U.S. Environmental Protection Agency, Washington D.C., EPA/600/R-99/030, March 1999. Also available at <http://www.epa.gov/asmdnerl/models3/doc/science/science.html>.
- Binkowski, F. S., and Shankar, U. (1995). The Regional Particulate Matter Model. I: Model Description and Preliminary Results, *J. Geophys. Res.* 100:26,191–26,209.
- Bott, A. (1989). A Positive Definite Advection Scheme Obtained by Nonlinear Renormalization of the Advection Fluxes, *Mon. Weather Rev.* 117:1006–1115.
- Dabdub, D., DeHaan, L., Kumar, N., Lurmann, F., and Seinfeld, J. H. (1998). *Computationally Efficient Acid Deposition Model for California*, Draft Report Contract #92-304, California Air Resources Board, Sacramento, CA.
- Dhaniyala, S., and Wexler, A. S. (1996). Numerical Schemes to Model Condensation and Evaporation of Aerosols, *Atmos. Environ.* 30:919–928.
- Fitzgerald, J. W., Hoppel, W. A., and Gelbard, F. (1998). A One-Dimensional Sectional Model to Simulate Multicomponent Aerosol Dynamics in the Marine Boundary Layer. 1. Modal Description, *J. Geophys. Res.* 103: 16,085–16,102.
- Fuchs, N. A., and Sutugin, A. G. (1971). High Dispersed Aerosols. In *Topics in Current Aerosol Research*, edited by G. M. Hidy and J. R. Brock. Pergamon Press, New York, pp. 1–60.
- Gelbard, F., and Seinfeld, J. H. (1980). Simulation of Multicomponent Aerosol Dynamics, *J. Colloid Interface Sci.* 78:485–501.
- Gelbard, F., Tambour, Y., and Seinfeld, J. H. (1980). Sectional Representation for Simulating Aerosol Dynamics, *J. Colloid Interface Sci.* 76:541–556.
- Harrington, D. Y., and Kreidenweis, S. M. (1998). Simulation of Sulfate Aerosol Dynamics. I. Model Description, *Atmos. Environ.* 32:1691–1700.
- Hudischewskij, A. B., and Seigneur, C. (1989). Mathematical Modeling of the Chemistry and Physics of Aerosols in Plumes, *Environ. Sci. Technol.* 23:413–421.
- Jacobson, M. Z. (1997a). Development and Application of a New Air Pollution Modeling System. II. Aerosol Module Structure and Design, *Atmos. Environ.* 31:131–144.
- Jacobson, M. Z. (1997b). Numerical Techniques to Solve Condensational and Dissolutional Growth Equations When Growth is Coupled to Reversible Reactions, *Aerosol Sci. Technol.* 27:491–498.
- Jacobson, M. Z., and Turco, R. P. (1995). Simulating Condensational Growth, Evaporation, and Coagulation of Aerosols Using a Combined Moving and Stationary Size Grid, *Aerosol Sci. Technol.* 22:73–92.
- Jaeger-Voirol, A., and Mirabel, P. (1989). Heteromolecular Nucleation in the Sulfuric Acid-Water System, *Atmos. Environ.* 23:2033–2057.
- Kerminen, V.-M., and Wexler, A. S. (1994). Post-Fog Nucleation of H₂SO₄-H₂O Particle in Smog, *Atmos. Environ.* 28:2399–2406.

- Lurmann, F. W., Wexler, A. S., Pandis, S. N., Musarra, S., Kumar, N., and Seinfeld, J. H. (1997). Modelling Urban and Regional Aerosols—II. Application to California's South Coast Air Basin, *Atmos. Environ.* 31:2695–2715.
- McMurry, P. H., and Friedlander, S. K. (1979). New Particle Formation in the Presence of an Aerosol, *Atmos. Environ.* 13:1635–1651.
- Meng, Z., Dabdub, D., and Seinfeld, J. H. (1998). Size-Resolved and Chemically Resolved Model of Atmospheric Aerosol Dynamics, *J. Geophys. Res.* 103:3419–3435.
- Meng, Z., and Seinfeld, J. H. (1996). Time Scales to Achieve Atmospheric Gas-Aerosol Equilibrium for Volatile Species, *Atmos. Environ.* 30:2889–2900.
- Pai, P., Vijayaraghavan, K., Seigneur, C., Hegarty, J., Leidner, M., and Louis, J.-F. (1998). *Particulate Matter Modeling in the Los Angeles Basin Using MM5 and SAQM-AERO—Preliminary Results. PM_{2.5} A Fine Particle Standard*, Vol. II, Air and Waste Management Association, Long Beach, CA, pp. 748–758.
- Pandis, S. N., Russell, L. M., and Seinfeld, J. H. (1994). The Relationship Between DMS Flux and CCN Concentration in Remote Marine Regions, *J. Geophys. Res.* 99:16,945–16,957.
- Raes, F. R., Saltelli, A., and Van Dingenen, R. (1992). Modeling Formation and Growth of H₂SO₄–H₂O Aerosols—Uncertainty Analysis and Experimental Evaluation, *J. Aerosol Sci.* 23:759–771.
- Seigneur, C. (1982). A Model of Sulfate Aerosol Dynamics in Atmospheric Plumes, *Atmos. Environ.* 16:2207–2228.
- Seigneur, C., Hudischewski, A. B., Seinfeld, J. H., Whitby, K. T., Whitby, E. R., Brock, J. R., and Barnes, H. M. (1986). Simulation of Aerosol Dynamics: A Comparative Review of Mathematical Models, *Aerosol Sci. Technol.* 5:205–222.
- Seigneur, C., Pai, P., Hopke, P., and Grosjean, D. (1999). Modeling Atmospheric Particulate Matter, *Environ. Sci. Technol.* 33:80A–86A.
- Seigneur, C., Wu, X. A., Constantinou, E., Gillespie, P., Bergstrom, R. W., Sykes, I., Venkatram, A., and Karamchandani, P. (1997). Formulation of a Second-Generation Reactive Plume and Visibility Model, *Air & Waste Manage. Assoc.* 47:176–184.
- Suck, S. H., and Brock, J. R. (1979). Evolution of Atmospheric Aerosol Particle Size Distributions via Brownian Coagulation: Numerical Simulation, *J. Aerosol Sci.* 10:581–590.
- Sun, Q., and Wexler, A. S. (1998). Modeling Urban and Regional Aerosols Near Acid Neutrality—Application to the June 24–25 SCAQS Episode, *Atmos. Environ.* 32:3533–3545.
- Tsang, T. H., and Brock, J. R. (1983). Simulation of Condensation Aerosol Growth by Condensation and Evaporation, *Aerosol Sci. Technol.* 2:311–320.
- Tsang, T. H., and Brock, J. R. (1986). Simulation of Condensation Aerosol Growth by Condensation and Evaporation, *Aerosol Sci. Technol.* 5:385–388.
- Tsang, T. H., and Huang, L. K. (1990). On a Petrov-Galerkin Finite Element Method for Evaporation of Polydisperse Aerosols, *Aerosol Sci. Technol.* 12:578–597.
- Varoglu, E., and Finn, W. D. L. (1980). Finite Elements Incorporating Characteristics for One-Dimensional Diffusion-Convection Equation, *J. Comp. Phys.* 34:371–389.
- Wexler, A. S., Lurmann, F. W., and Seinfeld, J. H. (1994). Modelling Urban and Regional Aerosols. I. Model Development, *Atmos. Environ.* 28:531–546.
- Wexler, A. S., and Seinfeld, J. H. (1990). The Distribution of Ammonium Salts Among a Size and Composition Dispersed Aerosol, *Atmos. Environ.* 24A:1231–1246.
- Whitby, E. R., and McMurry, P. H. (1997). Modal Aerosol Dynamics Modeling, *Aerosol Sci. Technol.* 27:673–688.
- Wu, X. A., Seigneur, C., and Bergstrom, R. W. (1996). Evaluation of a Sectional Representation of Size Distributions for Calculating Aerosol Optical Properties, *J. Geophys. Res.* 101:19277–19283.

Received February 8, 1999; accepted July 15, 1999.